The Seventh Asian-Pacific Symposium on Structural Reliability and Its Applications (APSSRA2020)
October 4–7 2020, Tokyo, Japan
T. Takada, I. Yoshida & T. Itoi (editors)

Estimation of Failure Probabilities for Steel Members Subjected to Fully Developed Fire and the Code-calibration for the Existing Fire Resistance Designs

X. Zhao[1] and F. Ozaki[2]

[1]*Grad. S. Environmental Studies, Nagoya Univ., D2-1(510), Furo-cho, Chikusa-ku, Nagoya-shi.*
Email: zhao.xiaomin@g.mbox.nagoya-u.ac.jp
[2]*Same as above. Email: ozaki@nuac.nagoya-u.ac.jp*

Abstract: The main purpose of this study is to estimate the failure probability of a protected steel member at fully developed compartment fire based on Eurocode 0, 1, and 3. For the parametric fire curve and advanced calculation model in Eurocode 1, the maximum temperatures of steel members in consideration of the dispersion of the fire loads are examined by the Monte Carlo method. According to the numerical results, the analytical parameters significantly affected the dispersion of the maximum temperature of steel members were clarified, and the relationships of the dispersion between the member temperature and the fire load were quantified. Furthermore, the failure probability of the steel member designed by Eurocode 0, 1 and 3 is examined, by the theoretical calculation model considering the uncertainty of the fire loads, dead and live loads and the strength of steel at the elevated temperatures, and the performance levels of the member optimally designed by the current design codes are clarified.

Keywords: fire resistance design of steel structure, variation of live fire load, parametric fire curve and advanced calculation model, failure probability of steel member at fire, Monte Carlo method.

1. Introduction

Performance-based fire resistance designs for steel building structures proposed by the Architectural Institute of Japan (hereinafter referred to as AIJ) and Eurocode 0, 1, 3 (hereinafter referred to as EC0, 1, 3) are used at practical fire safety designs. EC0, 1, 3 have been established by using the limit state design method based on the statistics and probability theory and provide the design framework based on the partial coefficient design method. However, regarding the fire resistance designs for both AIJ and EC, the fire loads, the variations of which mostly affect fire performances of structural members at fully developed compartment fire, are not directly considered as design parameters such as the partial safety coefficients and the load and resistance factors in verification methods on the fire resistance performance. It concludes that the effects of variations in fire loads on the steel member temperatures have not been quantified. Furthermore, since the verification methods on the fire safety of steel structures are, in many cases, established by expanding those on the structural safety at ambient temperature to elevated temperatures, it is very difficult to take the effects of the fire loads into account the load-bearing capacities of the members in the evaluation formulas at the fire resistance design. It is, therefore, necessary to clarify the relationship between the variation of the fire load and the maximum temperature of the steel member and to quantify the failure probability.

The main purpose of this study is to examine the failure probability for the protected steel member at the fully developed compartment fire evaluated by the EC0, 1, and 3, by using the theoretical probabilistic model proposed by the previous study (Ozaki, F. et al. 2018). This paper focuses on the simple fire evaluation model (parametric fire curve, hereinafter referred to as PF curve) and the advanced calculation model (hereinafter referred to as AF model) for the temperature-time curves under post-flashover conditions, which are proposed by the EC1, and the maximum temperatures of steel member by using the Monte Carlo method (hereinafter referred to as MC method) are estimated. Finally, to evaluate the performance levels required by the ECs and AIJ design, the code-calibrations on the steel member optimally designed by both codes are conducted.

2. Evaluation of Variations in Maximum Temperatures of Steel Members

To calculate the theoretical value of the failure probability for the protected steel member at the fire, it is necessary to quantify the relationships between the fire loads and the maximum temperatures of protected steel members at the fully developed compartment fires (Ozaki, F. et al. 2018). In this chapter, we quantify those relationships for both the PF and AF fire curves of EC1.

2.1 Evaluation of variations on *the steel member temperature based on PF curve*

2.1.1 Analytical conditions of PF curve

The PF curve is taken into account the essential physical phenomenon that affects the fire performance of post-flashover fire occurred in a compartment of moderate dimension and provided the simplified analysis expressions without sophisticated computer tools (European Committee for Standardization 2002).

To calculate the maximum temperature of the protected steel member under the PF curve, the fire compartment model with an opening is used. The numerical analyses based on the MC method considering the dispersion of fire load W_{load} [MJ/m^2] are conducted.

Table 1 shows the analytical parameters on the fire loads ($_{ave}W_{load}$: the average values, and $_{cov}W_{load}$: the coefficient of variations). The main parameters of the PF curve model are given by the fire load density $q_{t,d}$ [MJ/m^2], opening factor O [m$^{1/2}$], and the duration time t_{max} [h] of the heating phase at the fire, which are calculated by Eq. (1), (2) and (3), respectively.

Table 1. ${}_{ave}W_{load}$ and ${}_{cov}W_{load}$.

${}_{ave}W_{load}$ [MJ/m²]	250	500	750	1000
${}_{cov}W_{load}$	0.3, 0.5			

$$q_{t,d} = W_{load}\frac{A_f}{A_t} \tag{1}$$

$$O = \frac{A_v\sqrt{h_{eq}}}{A_t} \tag{2}$$

$$t_{max} = \frac{0.2 \times 10^{-3} \times q_{t,d}}{O} \tag{3}$$

Where

A_f is the surface area of the floor [m²];
A_t is the total surface area of enclosure [m²];
A_v is the total area of vertical openings in all walls [m²];
h_{eq} is the weighted average of window heights on all walls [m].

The analytical parameters except for the fire loads are given by the definite values, and those are shown in Table 2. The maximum duration time of the heating phase of the fuel controlled fire t_{lim} was given by t_{lim}= 5/12 [h] for the slow fire growth rate (European Committee for Standardization 2002). The applicable ranges of A_f, O, and $q_{t,d}$ for the PF curve are given by $A_f \le 500$ [m²], $0.02 \le O \le 0.20$ [m$^{1/2}$], $50 \le q_{t,d} \le 1000$ [MJ/m²], respectively, therefore, the value of $q_{t,d}$ is calculated by using the value of A_f = 423.18 [m²], which is close to the maximum value (= 500 [m²]). Each value of the opening factor O is determined by adjusting the value of the opening width L_{op}.

It is known that the fire load W_{load} follows a log-normal distribution in the case of the office occupancy in the building (AIJ 2017). On the other hand, for the analysis of the PF curve applied the log-normal distribution to the fire load, there is the possibility that the value of $q_{t,d}$ exceeds the above applicable range ($50 \le q_{t,d} \le 1000$ [MJ/m²]), depending on the variation of fire loads (${}_{cov}W_{load}$), and the effects that the parameter values out of the applicable range cause to the analytical results cannot be ignored. In particular, in the analytical case when the statistics on fire load are given by ${}_{ave}W_{load}$ = 250 [MJ/m²] and ${}_{cov}W_{load}$ = 0.5 (such as the practical office room), the probability of exceeding the lower limit value (50 [MJ/m²]) for $q_{t,d}$ is 0.157, which has a significant effect on the analytical result. To avoid this problem, it is assumed that the fire load W_{load} follows a shifted log-normal distribution with the lower-limit value derived from Eq. (1) using the lower limit-value of $q_{t,d}$, and the analytical results without the probability of the case of $q_{t,d}$ < 50 [MJ/m²] can be obtained. On the other hand, the possibility of exceeding the upper-limit value (1000 [MJ/m²]) of $q_{t,d}$ should be considered for the MC calculation using the shifted log-normal distribution. For instance, the analytical case when the average value (${}_{ave}W_{load}$) is large, the above possibility relatively becomes large, however, this value is sufficiently small as less than 0.01 even if the largest value of the variation of fire load is used (${}_{ave}W_{load}$ = 250 [MJ/m²] and ${}_{cov}W_{load}$ = 0.5).

The temperature of protected steel member is calculated by using the temperature evaluation formula proposed in the EC3. The cross section of the steel beam, the sectional shape factor H/A (AIJ 2017), and the protection material and its moisture content are H-400 × 200 × 8 × 13, 167[m^{-1}] (three-side heating), vermiculite plaster, and 15%, respectively. Furthermore, the fire protection thicknesses *di* are used as the parameters (10, 25, and 40 [mm]). To evaluate the maximum temperatures of protected steel member, the calculation is continued in the cooling phase after t_{max} for the PF curve, because of considering the thermal conduction in the protection material after the peak temperature of fire room.

Table 2. Analytical parameters.

Analytical parameters	Values
A_f [m²]	423.18
h_{room} [m]	4.00
h_{eq} [m]	3.50
A_t [m²]	1176
A_v [m²]	12.57, 69.12, 125.67
O [m$^{1/2}$]	0.02, 0.11, 0.20
$q_{t,d}$ [MJ/m²]	90, 180, 270, 360
L_{op} [m]	1.80, 9.87, 17.95

2.1.2 Numerical results of PF curve

Figs. 1 (a) and (b) show the analytical results on the standard deviations of the maximum temperature of steel member ${}_{std}T_s$. Those horizontal axes show the definite values of the maximum temperature of steel member ${}^{def}_{ave}T_s$, which were evaluated from the analyses without the variations of fire load. In this analysis, the average value ${}_{ave}W_{load}$ was used for the definitive value of fire load. In Figs. 1 (a) and (b), the three analytical results of the same colored and the same figured symbols connected by solid lines represent the analytical results of the different thicknesses of 10, 20, and 40 mm in descending order of horizontal axis ${}^{def}_{ave}T_s$, respectively. As shown in Figs. 1 (a) and (b), for the analytical results when those ${}^{def}_{ave}T_s$ are the same values (i.e., red ● and ○ marks at the same ${}^{def}_{ave}T_s$), those standard deviations of the steel temperature ${}_{std}T_s$ increase with increasing the coefficient of variation of fire load ${}_{cov}W_{load}$. On the other hand, for the analytical results at the same ${}_{cov}W_{load}$ values, the tendency of ${}_{std}T_s$ is complicated. That is, for the analytical results when the steel temperature ${}^{def}_{ave}T_s$ is below about 600 [K], those standard deviations ${}_{std}T_s$ increases with increasing that, however, the analytical results of ${}_{std}T_s$ are almost constant when ${}^{def}_{ave}T_s$ is above 700 [K] (Fig. 1 (a)). Furthermore, the different tendencies of ${}_{std}T_s$ are observed by changing the opening factor O.

Fig. 2 shows the relationships between the fire duration-time differences Δt and ${}_{std}T_s$ when the ventilation controlled fires occur. The fire duration-time difference Δt is given by the difference between the definite value of fire duration-time ${}^{def}_{ave}t_{max}$, which is calculated by using the average value of fire load, and the maximum duration time at the fuel controlled fire t_{lim} (5/12 [h]). If the value of Δt is negative, the fuel controlled fire occurred. On the other hand, when the value of Δt is sufficiently large (i.e., O = 0.02), the ventilation controlled fires occurred for all the analytical cases, and the value of ${}_{std}T_s$ in those cases were almost constant. Furthermore, in the case when the value of Δt approaches to 0, there is the possibility that either of the two combustion control types of ventilation or fuel controlled fire occurs, resulting in being the large value of ${}_{std}T_s$. This reason is as follows: the time-temperature relationship in the fuel controlled fire depends on the magnitude of fire load, on the other hand, the temperature during the heating phase of ventilation controlled does not depend on that. The evaluation models between the fuel and ventilation controlled fires are markedly different, and the fire temperatures evaluated from those models are different, in particular, when the combustion control type due to either ventilation or fuel controlled fires are frequently changed (this is, Δt ≈ 0, see Fig. 2).

As the variation of steel member temperature strongly depends on the difference of the combustion control type in this evaluation model. The steel member temperature at the fire can be easily evaluated by using the PF curve, however, at the same time, the evaluated fire curve at the practical design may be different from the actual fire because of occurring the different combustion type from the design, in particular, in the case when the value of Δt is close to 0 (see Fig. 2).

From the above discussion, it is inadequate to quantitatively evaluate the standard deviation of the steel member temperature in the case of considering the variation of the fire loads for the PF curves, because the evaluated fire curves are completely different according to the combustion types and the irregular standard deviations of steel member temperature are calculated.

2.2 Analysis of AF model

2.2.1 Analytical conditions of AF model

Regarding the AF model based on the EC1, a one-zone fire compartment model is exemplified as a calculation method, which is similar to the calculation model for the fully developed compartment fire used in the AIJ design. It is, therefore, assumed that the AF model is the same as that based on the AIJ design.

In other to establish the analytical model of the fire compartment room, the surface area of the floor A_f, fire compartment height h and opening height h_{op} are given by 1000 [m^2], 3.8 [m] and 1.5 [m], respectively, and the combustion controlled factor χ, which is denoted by the Eq.(4) (Himoto, K. et al. 2004), are used as the main parameters for the combustion type, and those values are given by 0.05, 0.08, and 0.1, respectively.

$$\chi \equiv \frac{A_{op}\sqrt{H_{op}}}{A_{fuel}} \tag{4}$$

Where

A_{op} is the area of openings [m^2];

H_{op} is the weighted average of the window heights on all the walls [m];

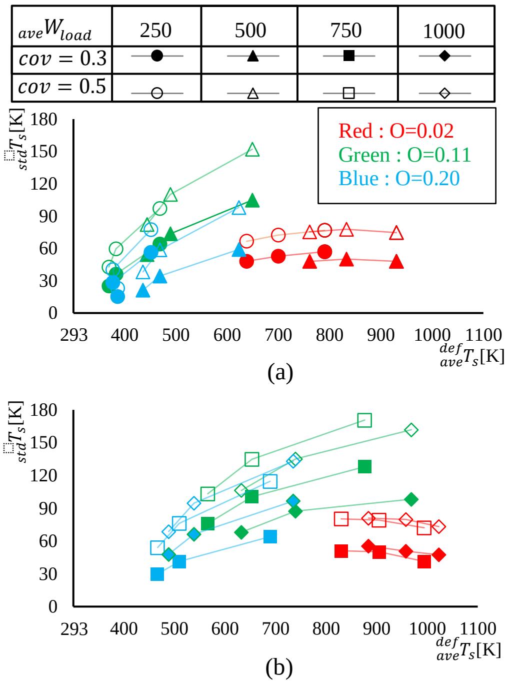

Figure 1. Relationships between ${}^{def}_{ave}T_s$ and ${}_{std}T_s$ in the cases of PF curve.

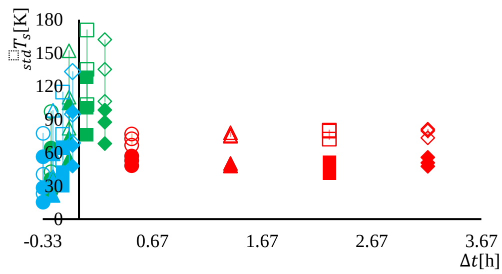

Figure 2. Relationships between Δt and ${}_{std}T_s$ in the cases of PF curve.

A_{fuel} is the surface area of all the combustible material in the fire compartment room [m^2].

According to the EC1, the statistics of the fire load follow the Gumbel type I distribution. It is, however, clarified that almost the same results on the variations (standard deviation) of the maximum temperatures of steel members are given even if the log-normal distribution is used instead of the Gumbel type I distribution (Zhao, X. et al. 2019). Therefore, for the AF model based on the EC1, it is assumed that the fire load follows the log-normal distribution. The average values (${}_{ave}W_{load}$) and the coefficient of variation (${}_{cov}W_{load}$) for the fire load are given by 250, 500 [MJ/m^2], and 0.3, 0.5, respectively.

Regarding the calculation of the maximum steel member temperatures, the evaluation equation proposed by the EC3 is used. The protection material was equivalent to sprayed mineral fiber, and the water content was 15%. The coating thickness di and the sectional shape factor (H/A) were used as the analytical parameters, and given by 20, 25, 30 [mm], and 134, 167, 194 [m^{-1}], respectively.

2.2.2 Numerical results of AF model

Fig. 3 shows the relationships between the definite values of the maximum steel member temperature ${}^{def}_{ave}T_s$ and the average values of the maximum steel member temperature ${}^{MC}_{ave}T_s$ obtained by the MC analyses. As shown in Fig.3, ${}^{def}_{ave}T_s$ and ${}^{MC}_{ave}T$ are matched well for all the analytical cases. Therefore, it concludes that the average values of maximum steel member temperature can be evaluated by the definite values ${}^{def}_{ave}T_s$, which are calculated from the average values of fire load.

Fig. 4 shows the relationships between the definite values ${}^{def}_{ave}T_s$ and the standard deviations of the maximum steel member temperature ${}_{std}T_s$ obtained by the analyses of the MC method. As shown in Fig. 4, the analytical results are plotted on almost the same curve in the case of the same coefficient of variation, regardless of the average values of fire load, the thicknesses of protection material, the combustion controlled factor and the cross-sectional shapes, which is the same tendency as the previous study (Ozaki, F. et al. 2018). An approximate curve for those numerical results is obtained by the following Eq. (5), which gives the relationships between the variation of fire load and that of the maximum member temperature, which is the essential relationship to calculate the theoretical value of the fracture probability for the steel member at the fire.

$$
\begin{aligned}
{}_{std}T_S = \Delta Ts \Bigg\{ & \frac{\Delta Ts - 787}{1067}\left(3\,{}_{cov}W_{load}^{\;3} - 2.5\,{}_{cov}W_{load}^{\;2} - 1.07\,{}_{cov}W_{load} - 0.015\right) \\
& + \frac{\Delta Ts - 247}{1700}\left(-\,{}_{cov}W_{load}^{\;2} + 2.4\,{}_{cov}W_{load} - 0.03\right)\Bigg\}
\end{aligned}
\qquad (5)
$$

Where

ΔTs is the difference between the definite value of the maximum temperature of steel member and the ambient temperature (that is, the increase of gas temperature due to fire) [°C].

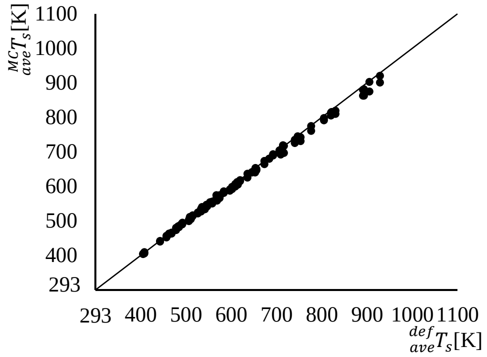

Figure 3. Relationships between ${}^{def}_{ave}T_s$ and ${}^{MC}_{ave}T_s$ in the cases of AF model.

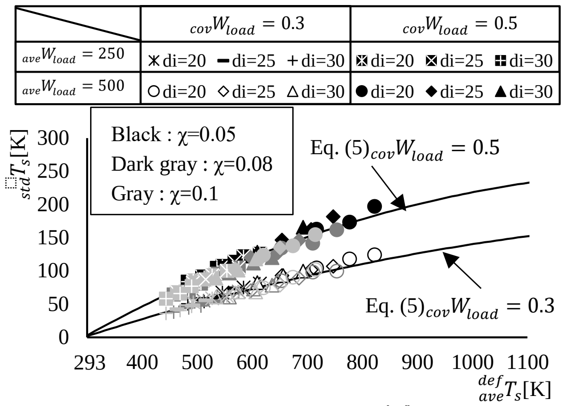

Figure 4. Relationships between ${}^{def}_{ave}T_s$ and ${}_{std}T_s$ in the cases of AF model.

3. Code-calibration

In order to clarify the difference between the fire resistance performance levels required by the EC and AIJ design, the failure probability of steel members designed by each code is evaluated, and the code-calibration for the two codes is conducted. It is assumed that the steel member in the fully developed compartment fire is designed to be satisfied with the minimum required performance regarding each design code. The failure probability of the steel member is evaluated by using the theoretical failure probability formula (Eq. (6)) proposed in the reference (Ozaki, F. et al. 2018).

$$P_f = \int_0^\infty f_S(s)\left[\int_0^\infty \left[\int_0^s f_{\bar{R}}\left(\frac{\bar{r}}{\kappa(t)}\right)d\bar{r}\right]\cdot\frac{f_T(t)}{\kappa(t)}dt\right]ds \qquad (6)$$

Where,

$f_S(s)$ is the probability density function of the vertical load applied to the steel member;

$f_{\bar{R}}(\bar{r})$ is the probability density function of the resistant strength at the ambient temperature;

$f_T(t)$ is the probability density function of the maximum member temperatures at the temperature t;

$\kappa(t)$ is the reduction factor of the steel at the elevated temperature based on the coupon test results, which is evaluated from the average values at each temperature.

To conduct the code-calibration using the above Eq. (6), the relationships between the design and average values for the fire load, the maximum steel member temperature, the applied vertical loads, and the steel strength must be quantified, and are given below.

3.1 Code-calibration for fire resistance design

3.1.1 Relationships between the design and average values for the fire load and the maximum steel member temperatures

The design and average values of fire load are given as shown in Table 3. In the general fire resistance design, the design value of the fire load is larger than the average value, therefore, the member temperature evaluated based on each design code is lower than that calculated from the average value of fire load. When evaluating the failure probability based on the Eq. (6) of the theoretical equation constructed by each average value, the formulation of the relationship between the design value ${}_dT_s$ and the average value ${}_rT_s$ for the maximum steel member temperature is required. To obtain this relationship, the parametric calculations were performed with the various fire compartment and steel member models, as the results, the relationship between ${}_dT_s$ and ${}_rT_s$ for each design code was obtained by Eq. (7), (8), and (9), which is an approximately linear function of the calculation results.

Table 3. Design conditions of fire load.

Occupancy	Design code	Average value [MJ/m^2]	Coefficient of variation	Design value [MJ/m^2]
Office	EC	420	0.3	504
	AIJ			672

$$ {}_{r}T_{s,PF} = 0.90\ {}_{d}T_{s} \quad (7) $$

$$ {}_{r}T_{s,AF} = 0.83\ {}_{d}T_{s} \quad (8) $$

$$ {}_{r}T_{s,AIJ} = 0.71\ {}_{d}T_{s} \quad (9) $$

The probability density function of the maximum member temperature is assumed to follow the log-normal distribution for both EC and AIJ design, and the average values of the maximum temperature of steel member ${}_{r}T_{s}$ are obtained from the above Eq. (7) to (9), and the standard deviations are obtained from Eq. (5) (ECs) and the past study (AIJ design; Ozaki, F. et al. 2018), respectively.

3.1.2 Relationships between the design and average values for the steel strength

The steel material is JIS SN400 steel grade, and the design values of the steel strength at the elevated temperature are obtained by ${}_{d}\kappa({}_{d}t\ )\cdot{}_{d}\bar{\sigma}_{y}$, where ${}_{d}\kappa({}_{d}t_{cr})$ is the design reduction factor of the steel strength at the temperature ${}_{d}t_{cr}$ defined by each design code, and ${}_{d}\bar{\sigma}_{y}$ is the design steel strength at the ambient temperature (= 235 [N/mm^2]). On the other hand, the average values of steel strength at the elevated temperature are evaluated by $\kappa(t)\cdot{}_{ave}\bar{\sigma}_{y}$, where $\kappa(t)$ is the reduction factor of the average steel strength evaluated from the past coupon test results, and ${}_{ave}\bar{\sigma}_{y}$ is the average steel strength at the ambient temperature (= 292 [N/mm^2]). Furthermore, it is assumed that the steel strength at the high temperature follows the log-normal distribution and the coefficient of variation for that is given by 0.1 regardless of the temperature.

3.1.3 Relationships between the design and average values for the applied vertical loads

For the design values of the applied vertical load combined the lived with dead load in the case of the AIJ design, the safety factors of the lived and dead loads are evaluated by 2.49 and 1.0, respectively, according to the previous study (Zhao, X. et al. 2018). The design value of the applied load E_{AIJ} is evaluated by the average values of both loads (Q_r and G_r; Eq. (12)). On the other hand, for the combined loads regarding the lived and dead loads of the EC0, the design values E_d and $E_{fi,d}$ denoted by the structural design at the ambient temperature and the fire design are used, respectively, which are given by $E_d = \gamma_G\cdot G_k + \gamma_Q\cdot Q_k$ and $E_{fi,d} = G_k + \varphi_{2,1}Q_k$, respectively, by using the characteristic values of both lived and dead loads (Q_k and G_k), the partial factors (γ_G, γ_Q), and the quasi-permanent factor $\varphi_{2,1}$ (European Committee for Standardization 2005a).

By replacing the average values of lived and dead loads (Q_r and G_r) with those characteristic values Q_k and G_k in the above equations, both Eq. (10) and (11) are obtained as the design values of applied vertical loads $E_{fi,d}$ and E_d for the fire design and the structural design at the ambient temperature, respectively, where $\varphi_{2,1}$, γ_Q and γ_G for $E_{fi,d}$, and γ_Q and γ_G for E_d are given by 0.6, 1.0, 1.0, 1.5, and 1.35, respectively (European Committee for Standardization 2005a).

$$ E_{fi,d} = G_r + Q_r \quad (10) $$

$$ E_d = 1.35\cdot G_r + 2.5\cdot Q_r \quad (11) $$

$$ E_{AIJ} = G_r + 2.49\cdot Q_r \quad (12) $$

3.2 Code-calibration results

Fig. 5 and 6 show the relationships between the failure probabilities of the steel member at the fire, which are indicated by the reliability index β, and the temperatures of the design point T_G evaluated from each design code. The horizontal axis T_G is the temperature when the design value of maximum temperature for the protected steel member is equal to that of the collapse temperature, that is, the steel member is optimally designed so as to be satisfied with the minimum required performance based on each design code. The analytical results on the EC are shown in Fig. 5 and 6, when the design values of applied loads $E_{fi,d}$ and E_d for the fire (Fig. 5) and the structural design (Fig. 6) are used, respectively.

As shown in Fig. 5, the results in the case of using the PF curve (solid line) and the AF model (broken line) exhibit very higher failure probabilities than the AIJ design (dotted line), and the probabilistic fire-resistant performances of the formers are very insufficient. For the ECs, the design reduction factor of the steel strength ${}_{d}\kappa({}_{d}t_{cr})$ is close to that based on the average values, furthermore, the resistance factor in the design equation at the fire situation is given by 1.0, and the design value of the lived load is used as that average value. For those reasons, the failure probability becomes higher as shown in Fig. 5, and the margin of the fire safety for the steel structural members is extremely insufficient in the case of the ECs.

On the other hand, as shown in Fig. 6, when the steel member is designed by the design value of the applied load in the structural design at the ambient temperature E_d, that failure probability exhibits the low value at the low fire temperature (20 – 300 [℃]), however, in the high-temperature region, the failure probabilities of both the PF and AF curves become higher, such as the case of using the applied load for the fire $E_{fi,d}$.

4. Conclusions

In this paper, the failure probability of steel member at the fully developed compartment fire designed by EC0, 1, and 3 is quantified by considering the uncertainty of the fire loads, the lived and dead loads, and the strength of steel at the elevated temperatures, respectively. Furthermore, the code-calibration was performed for the fire resistance design based on the EC0, 1, 3, and the AIJ design,

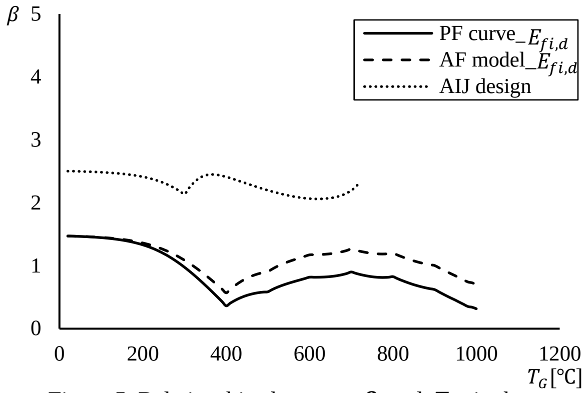

Figure 5. Relationships between $\boldsymbol{\beta}$ and $\boldsymbol{T_G}$ in the cases when $\boldsymbol{E_{fi,d}}$ of EC are used

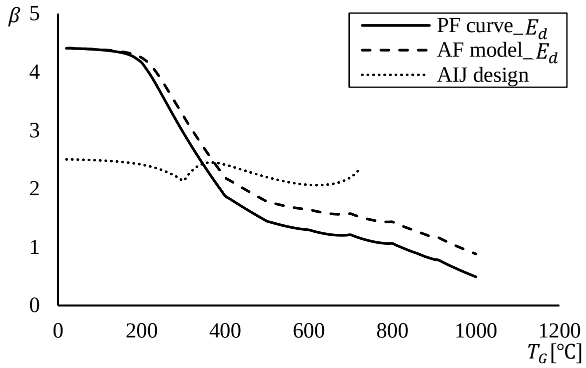

Figure 6. Relationships between $\boldsymbol{\beta}$ and $\boldsymbol{T_G}$ in the cases when $\boldsymbol{E_d}$ of EC are used

respectively. The failure probability of the steel member designed by the EC0, 1, and 3 exhibited very higher values. Furthermore, the required performance level for the steel member optimally designed by the above design codes depend on the temperature of design point T_G, which means that controlling the failure probability at the practical design is very difficult.

In order to establish the limit state design using the target reliability index for the fire resistance design, the design method based on the probabilistic performance-based design in the fire situation should be developed.

References

European Committee for Standardization. 2005a. *EN 1990 (2002) (English): Eurocode - Basis of structural design*.

European Committee for Standardization. 2002. *EN 1991-1-2 (2002) (English): Eurocode 1: Actions on structures – Part 1-2: General actions - Actions on structures exposed to fire*.

European Committee for Standardization. 2005b. *EN 1993-1-2 (2005) (English): Eurocode 3: Design of steel structures – Part 1-2: General rules – Structural fire design*.

Architectural Institute of Japan. 2017. *Recommendation for Fire Resistant Design of Steel Structure (in Japanese).*

Ozaki, F., Tezuka, K., Mori, Y. 2018. Estimation on failure probability of a steel member at fully-developed compartment fire. In *Journal of Structural and Construction Engineering. Transactions of AIJ*, Vol.83, No.753, 1725-1733pp, Nov., 2018 (in Japanese).

Zhao, X., Ozaki, F., Mori, Y. 2019. Verification of steel member temperatures considering dispersion of fire loads - Analytical verification results using parametric fire curves proposed by Eurocode -. *Summaries of Technical Papers of Annual Meeting, Architectural Institute of Japan (Hokuriku)*, Sept., 2019 *(in Japanese)*.

Himoto, K., Tanaka, T., 2004. A Burning Model for Charring Materials and Its Application to the Compartment Fire Development. *Fire Science and Technology*, Vol.23, No.3, 170-190pp, 2004.

Zhao, X., Tezuka, K., Ozaki, F. 2018. Estimation on failure probability of a steel structure member subjected to fully-developed compartment fire and code-calibration. *Summaries of Technical Papers of Annual Meeting, Architectural Institute of Japan (Tohoku)*, July, 2018 *(in Japanese).*